Available online at www.sciencedirect.com

ScienceDirect

Mendeleev Commun., 2021, **31**, 132–134

Mendeleev Communications

Interaction between laminar flames of natural gas–oxygen mixtures and planar obstacles with asymmetrical openings

Nikolai M. Rubtsov,*[a] Victor I. Chernysh,[a] Georgii I. Tsvetkov[a] and Kirill Ya. Troshin[b]

[a] *A. G. Merzhanov Institute of Structural Macrokinetics and Materials Science, Russian Academy of Sciences, 142432 Chernogolovka, Moscow Region, Russian Federation. E-mail: nmrubtss@mail.ru*

[b] *N. N. Semenov Institute of Chemical Physics, Russian Academy of Sciences, 119991 Moscow, Russian Federation*

DOI: 10.1016/j.mencom.2021.01.043

It was experimentally shown that the flame penetration limit, expressed by the diameter of the orifice, is less for a single asymmetrical obstacle (< 15 mm under our conditions) than for a single symmetrical obstacle (20 mm). It was revealed that the penetration limit increases with an increase in the number of obstacles with asymmetrical openings.

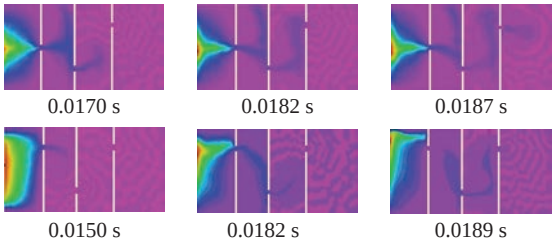

Keywords: ignition, laminar flame, flame penetration limit, planar obstacle, asymmetrical opening, orifice, Navier–Stokes equations.

In many practical applications, the possible consequences of a large-scale accidental release of flammable gas or vapor must be taken into account. The risk of a large explosion is a major hazard that must be adequately assessed as an integral part of the design process for any new installation or operating procedure.[1] Making reasonable predictions of the effects of an accidental explosion is a difficult task due to the complexity of the physical and chemical processes involved. There are no reliable scaling laws that can be used to relate small-scale experimental tests to full-scale explosion behavior.[2–4] Full-scale experimental testing is often impracticable or prohibitively expensive, or both. Current industrial practice in explosion modelling is generally based on a rational simplification of the plant geometry while maintaining the principal physical features as much as possible. These models can be run very quickly on standard desktop computers, which means that a large number of explosion cases and technological room designs can be analyzed in a very short time.

The governing equations for the simulation of gas explosions are the reacting compressible Navier–Stokes equations. However, when modelling explosions in pipes,[5] technological rooms, combustion chambers and chemical reactors that are volumes of complex geometry, it is necessary to have reliable experimental data. Modelling turbulent deflagration combustion of premixed gas mixtures in a closed space of complex geometry is a challenging problem, especially in connection with the need to adequately represent a reaction zone, which presupposes some experiment. In this regard, modelling in small volumes at pressures below atmospheric is very desirable to anticipate the effects expected for a large scale, and it is also much cheaper.[6] Besides, such modelling allows one to determine whether a large-scale natural experiment at atmospheric pressure could pose a hazard to the integrity of the installation and the lives of personnel.[7]

In gas explosions occurring in process industries, the number and location of openings in obstacles, along with, for example, the shape of the obstacle, the size of the relative opening, *etc.*, are key parameters that determine the intensity of such explosions.[8,9] Very limited information on the contribution of these parameters is documented.[10]

We have shown earlier[10] that the features of the penetration of diluted methane–oxygen flames through planar and spherical obstacles are mostly determined by gas-dynamic processes. However, the kinetic mechanism of combustion should also be considered. For example, flame turbulization can determine the kinetics of combustion, including the transition of low-temperature combustion of hydrocarbons to a high-temperature mode.[11] We showed that the flame after a single obstacle does not arise in the immediate vicinity of the obstacle, and the primary centre of ignition is observed at some distance from the obstacle surface (flame jump). Two or more closely located flat obstacles considerably suppress the flame propagation. The length of the flame jump after the opening in an obstacle is primarily determined by the time of the transition from laminar to turbulent flow rather than the time of ignition delay.

This work was aimed at identifying the patterns of flame penetration through flat obstacles arranged in such a way that the openings of neighbouring obstacles are not coaxial to each other. Experimental data were modelled to determine the effect of the obstacles on the flame penetration process compared to the flat obstacles with the openings arranged along the reactor axis. It is also relevant to provide a safe arrangement of the openings between neighbouring technological rooms. The experimental results are compared to combustion simulations.†

First, a limit value for the diameter of a single central opening was determined. It was 20 mm for our installation at a total pressure of 180 Torr in accordance with published data.[10] The results of high-speed filming of the FF propagation in the combustible mixture at an initial pressure of 180 Torr through flat obstacles with a diameter of 14 cm with differently arranged openings are presented in Figure 1. Figure 1(*a*) shows a typical sequence of frames of flame penetration through two asymmetrical circular openings with a diameter of 22 mm, which is above the penetration limit, with the sequence *1* of frames corresponding

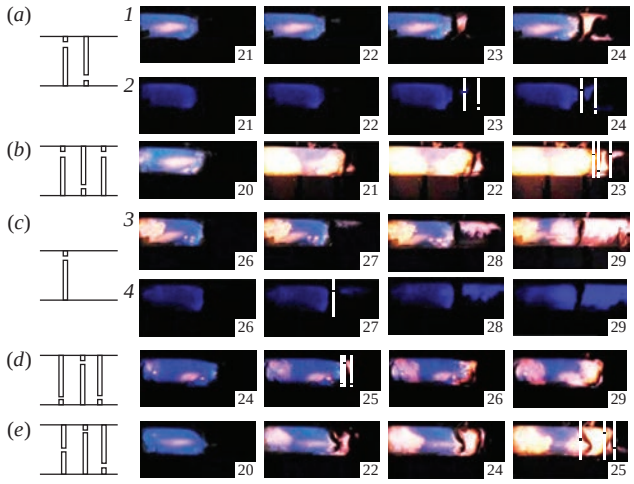

Figure 1 Frame sequences of high-speed filming of FF propagation through (*a*) two asymmetrical circular openings of 22 mm in diameter (*1*) without and (*2*) with an optical filter, (*b*) three asymmetrical circular openings of 22 mm in diameter without an optical filter, (*c*) a single asymmetrical opening of 15 mm in diameter (*3*) without and (*4*) with an optical filter, (*d*) three asymmetrical circular openings of 15 mm in diameter without an optical filter, and (*e*) one symmetrical circular opening and two asymmetrical circular openings of 15 mm in diameter without an optical filter. The interference filter with a bandpass of 435 ± 15 nm was used as an optical filter. The initial pressure was 180 Torr. The figures on each frame correspond to the frame number after initiating discharge. The frame rate was 600 s^{-1}. The configurations of obstacles are shown schematically on the left of the Figure as well as in the several frames (white vertical lines). A flame propagated from left to right.

to the absence of an optical filter. In the sequence *2* of frames [see Figure 1(*a*)], the interference filter with a bandpass of 435 ± 15 nm is placed in front of the camera, *i.e.*, the distribution of CH radicals during flame propagation is visualized. Further, we showed that the flame penetrates through three asymmetrical circular openings with a diameter of 22 mm as well [Figure 1(*b*)]. It was also found that the flame penetrates through two asymmetrical circular openings with a diameter of 19 mm, but does not penetrate through three asymmetrical circular openings with a diameter of 19 mm.

Figure 1(*c*) displays a typical sequence of frames of flame penetration through a single asymmetrical opening with a diameter of 15 mm, with the sequence *3* of frames corresponding to the absence of optical filters. In the sequence *4* of frames [see Figure 1(*c*)], the interference filter with a bandpass of 435 ± 15 nm is placed in front of the camera lens. As can be seen, the value of the diameter is less than the critical diameter of the flame penetration limit through a single central opening, *i.e.*, the flame penetrates through the asymmetrical opening of a subcritical diameter compared to the symmetrical case.

Figure 1(*d*) presents the typical frame sequences of high-speed filming of FF propagation through three asymmetrical circular openings with a diameter of 15 mm. It should be noted that the flame does not penetrate through the two asymmetrical openings with a diameter of 15 mm. However, the penetration can be achieved by replacing the first obstacle with an asymmetrical opening of 15 mm in diameter by an obstacle with a symmetrical opening of 15 mm in diameter. Figure 1(*e*) demonstrates typical sequences of frames of flame penetration through a complex obstacle consisting of one symmetrical circular opening and two asymmetrical circular openings of 15 mm in diameter, which illustrate the aforesaid.

Note that since the obstacles are not rigidly fixed, they are shifted under the action of hot products of a propagating flame, and the shift is more pronounced if the flame does not penetrate through the set of obstacles.

From the above experiments, we conclude that the flame penetration limit, expressed by the diameter of the orifice, is less for a single asymmetrical obstacle (<15 mm under our conditions) than for a single symmetrical obstacle (20 mm) under the same conditions. It is shown that the limit of flame penetration through a set of obstacles increases with an increase in the number of obstacles with asymmetrical openings of the same diameter. In this case, the penetration limit for two and three asymmetrical obstacles can be reduced by replacing the first obstacle in the direction of flame propagation by an obstacle with a symmetrical opening.

We attempted to reproduce the penetration of a flame through the obstacles by numerical simulation using the compressible reactive Navier–Stokes equations in the low Mach number approximation in a dimensionless form,[12] describing the propagation of a flame in a two-dimensional channel. Earlier, the equations showed qualitative agreement with experiments.[10] The problem was solved by the finite element analysis.[‡] A simple chain mechanism[10] was used. The initiation condition was taken as $T = 10$ at the left boundary of the channel in which there was an obstacle. The boundary conditions, including the orifice, were $C_\xi = 0$, $u = 0$, $v = 0$, $p_\xi = 0$ as well as a convective heat exchange $T_t = T - T_0$, where ξ is the dimensionless coordinate.

The results of qualitative calculations of flame propagation through complex obstacles are shown in Figures 2 and 3. As can be seen, the results of the analysis are in qualitative agreement with the experiment shown in Figure 1. Indeed, the calculated

[†] In the experiments, flame propagation in the stoichiometric mixtures of methane and oxygen diluted with CO_2 and Ar was investigated at initial pressures of 150–200 Torr and initial room temperature in a horizontal cylindrical quartz reactor with a length of 70 cm and a diameter of 14 cm. The reactor was fixed in stainless steel gateways at the butt-ends, which were equipped with gas inlets for pumping and blousing, as well as a safety shutter, which swung outward when the total pressure in the reactor exceeded 1 atm.[10] Two spark ignition electrodes were placed near the left butt-end of the reactor.[10] Thin obstacles with a diameter of 140 mm having circular openings with a diameter of 22, 19 and 15 mm were placed vertically in the center of the reactor in the ways shown in Figure S1 (see Online Supplementary Materials). In most experiments, the openings in the obstacles were located asymmetrically relative to the reactor axis (40 mm from the center). One, two and three obstacles with the same diameter of the opening were placed in the reactor (see Figure S1). In the case of two or three obstacles in the reactor, the distance between them was 40 mm. In some experiments, the first obstacle in the direction of flame propagation had a single symmetrical opening of the appropriate diameter [Figure 1(*e*), left].

The combustible mixture (15.4% CH_4 + 30.8% O_2 + 46% CO_2 + 7.8% Ar) was prepared in advance. CO_2 was added to enhance the quality of filming by reducing the velocity of the flame front (FF). Ar was added to decrease the discharge threshold.[10] The reactor was filled with the mixture to the required pressure. Then spark ignition was performed, while the discharge energy was 1.5 J.

Speed filming of ignition dynamics and FF propagation[10,11] was carried out from the side of the reactor with two Casio Exilim F1 Pro digital cameras with a frame rate of 600 s^{-1}. An interference filter with a central wavelength of 435 nm, a filter factor of 40% and a half-bandwidth of 15 nm was applied to select the emission of CH ($A^1\,\Delta$–$X^2\,\Pi$) at 431 nm.[11] The video file was stored in the computer's memory, and its time-lapse processing was performed. Chemically pure reagents were used.

The blocking ratio (BR) of a single orifice with a round opening was applied to consider the process of the flame quenching. It was calculated by the equation: $BR = 1 - (d/D)^2$, where d and D denote the inner diameter of the orifice and tube, respectively. In this work, the obstacles with openings with a diameter of 22, 19 and 15 mm and BR of 0.975, 0.981 and 0.989, respectively, were examined.

[‡] The FlexPDE software package was used (FlexPDE 6.08, 1996–2008 PDE Solutions Inc.[13]).

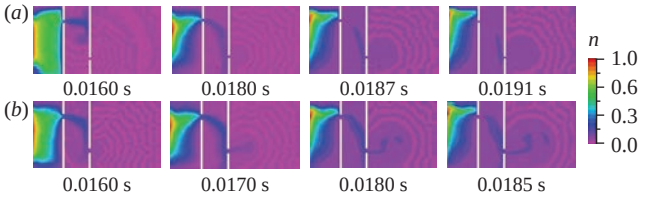

Figure 2 Maps of calculated dimensionless concentration (n) of the intermediate centre for flame penetration through two asymmetrical openings with a diameter of (*a*) 0.02 and (*b*) 0.04 of the channel diameter at various times after ignition. The scale of n is presented on the right.

dimensionless concentration (n) of the intermediate center for flame penetration through two asymmetrical openings indicates that the flame does not penetrate through two obstacles with asymmetrical openings with smaller slits [BR = 0.9996, Figure 2(*a*)], but it penetrates through two asymmetrical openings with larger slits [BR = 0.9984, Figure 2(*b*)], which is in qualitative agreement with our experimental results.

According to in Figure 3, the flame penetrates through one symmetrical slit and two asymmetrical slits but does not penetrate through three asymmetrical slits, while the slits in all obstacles have the same size. The result obtained qualitatively agrees with the experimental data presented in Figures 1(*d*),(*e*). It should be noted that agreement is reached on the final result, namely, whether the flame can penetrate through the set of obstacles. It may be, in particular, because in the numerical model, obstacles are rigidly fixed, but in the experiment, they can move being nonrigidly sealed by means of polymer material.[14] Thus, in applications with low-speed turbulent combustion, the low Mach number approximation of the reactive Navier–Stokes equations is a suitable basis for qualitative simulation.

In summary, it was experimentally shown that the flame penetration limit expressed by the diameter of the orifice is less for a single asymmetrical obstacle (<15 mm under our conditions) than for a single symmetrical obstacle (20 mm). It was revealed

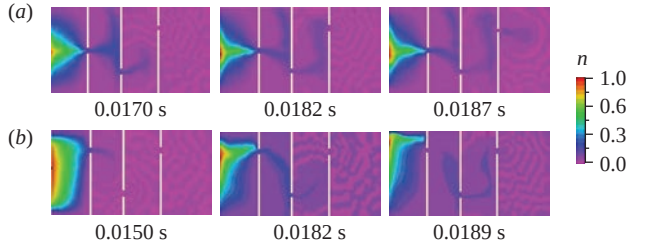

Figure 3 Maps of calculated dimensionless concentration (n) of the intermediate centre for flame penetration through (*a*) one symmetrical and two asymmetrical openings as well as (*b*) three asymmetrical openings at various times after ignition. The diameter of the openings is 0.04 of the channel diameter. The scale of n is presented on the right.

that the penetration limit increases with an increase in the number of obstacles with asymmetrical openings. In this case, the penetration limit for two or three asymmetrical obstacles can be reduced by replacing the first obstacle in the direction of flame propagation with an obstacle with a symmetrical opening. It was shown that in applications with low-speed turbulent combustion, the low Mach number approximation of the reactive Navier–Stokes equations is a suitable basis for qualitative simulation. The results of this work are important to provide a safe arrangement of the openings between the neighbouring technological confinements.

Online Supplementary Materials

Supplementary data associated with this article can be found in the online version at doi: 10.1016/j.mencom.2021.01.043.

References

1 J. R. Petrie, *Piper Alpha Technical Investigation: Interim Report*, Department of Energy, London, 1988.
2 W. P. M. Mercx, D. M. Johnson and J. Puttock, *Process Saf. Prog.*, 1995, **14**, 120.
3 J. S. Puttock, M. R. Yardley and T. M. Cresswell, *J. Loss Prev. Process Ind.*, 2000, **13**, 419.
4 K. E. Rian, T. Evanger, B. E. Vembe, N. I. Lilleheie, B. Lakså, B. H. Hjertager and B. F. Magnussen, *Chemical Engineering Transactions*, 2016, **48**, 175.
5 F. Lees, *Lees' Loss Prevention in the Process Industries: Hazard Identification, Assessment and Control*, 4th edn., Butterworth-Heinemann, 2012.
6 S. R. Gubba, S. S. Ibrahim, W. Malalasekera and A. R. Masri, *Combust. Sci. Technol.*, 2008, **180**, 1936.
7 N. M. Rubtsov, V. I. Chernysh, G. I. Tsvetkov and K. Ya. Troshin, *Mendeleev Commun.*, 2019, **29**, 108.
8 J. Kindracki, A. Kobiera, G. Rarata and P. Wolanski, *J. Loss Prev. Process Ind.*, 2007, **20**, 551.
9 V. Akkerman, V. Bychkov, A. Petchenko and L.-E. Eriksson, *Combust. Flame*, 2006, **145**, 675.
10 N. M. Rubtsov, *The Modes of Gaseous Combustion*, Springer, 2016.
11 N. M. Rubtsov, A. N. Vinogradov, A. P. Kalinin, A. I. Rodionov, K. Ya. Troshin, G. I. Tsvetkov and V. I. Chernysh, *Mendeleev Commun.*, 2017, **27**, 192.
12 A. Majda, *Equations for Low Mach Number Combustion*, Center of Pure and Applied Mathematics, University of California, Berkeley, 1982, report no. 112.
13 G. Backstrom, *Simple Fields of Physics by Finite Element Analysis*, GB Publishing, Malmö, Sweden, 2005.
14 M. I. Alymov, N. M. Rubtsov, V. I. Chernysh, G. I. Tsvetkov and K. Ya. Troshin, *Mendeleev Commun.*, 2017, **27**, 387.

Received: 5th October 2020; Com. 20/6326